Electronic Supplementary Material (ESI) for Journal of Materials Chemistry A.

Supporting Information for:

Surfactant dependent flower and grass like $Zn_{0.76}Co_{0.24}S/Co_3S_4$ for high-performance all-solid-state asymmetric supercapacitors

Yuan Yang,[a] Wei Huang,[b] Shuo li,[a] Lijie Ci,[a] Pengchao Si*[a]

[a]SDU & Rice Joint Center for Carbon Nanomaterials, MOE Key Laboratory for Liquid-Solid Structural Evolution and Processing of Materials, School of Materials Science and Engineering, Shandong University, Jinan 250061, P. R. China
[b]Department of Chemistry, Technical University of Denmark, DK-2800 Kongens Lyngby, Denmark

Corresponding authors:
*Pengchao Si: pcsi@sdu.edu.cn

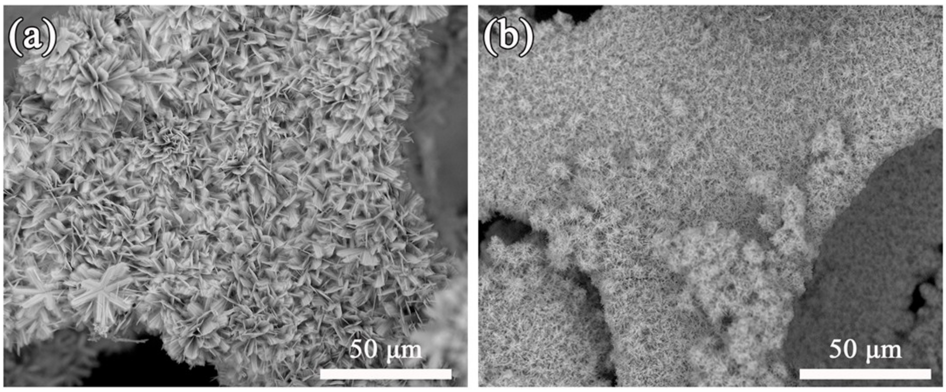

Fig. S1 Low magnification SEM images of (a) flower and (b) grass like $Zn_{0.76}Co_{0.24}S/Co_3S_4$.

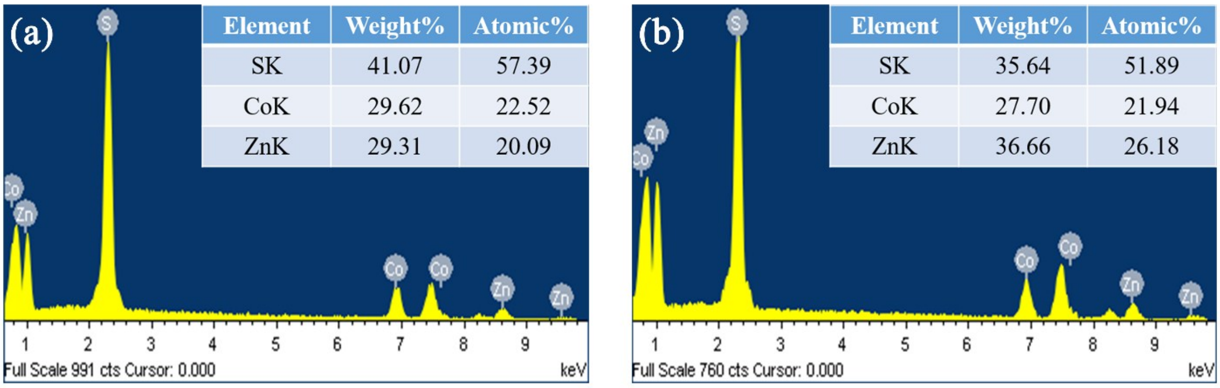

Fig. S2 EDS spectrum of (a) flower and (b) grass like $Zn_{0.76}Co_{0.24}S/Co_3S_4$.

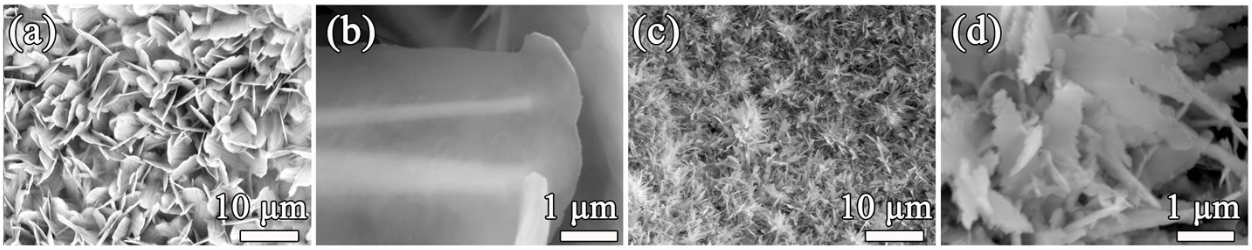

Fig. S3 SEM images of (a and b) flower and (c and d) grass like ZN-Co precursors.

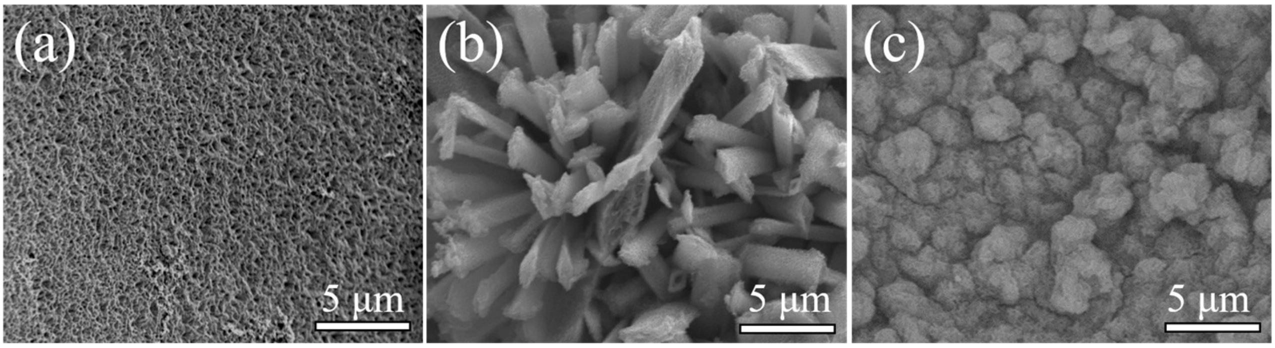

Fig. S4 SEM images of (a) no-surfactant, (b) NH_4F-0.37, (c) PVP-0.5 $Zn_{0.76}Co_{0.24}S/Co_3S_4$.

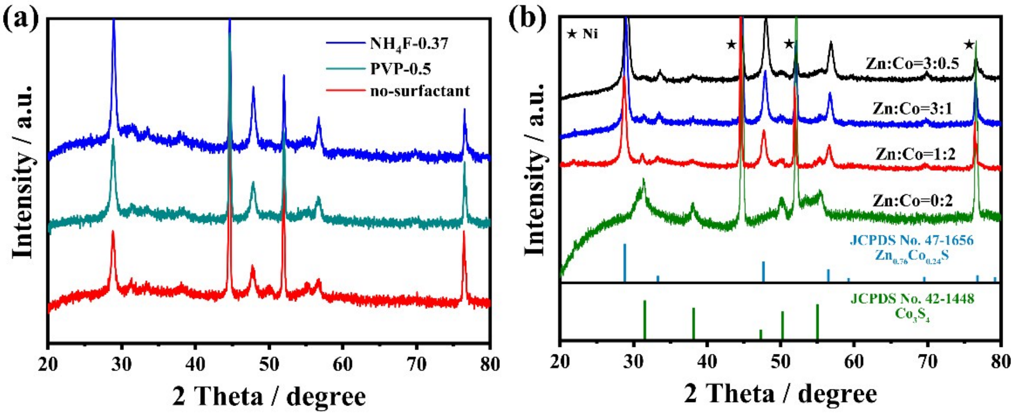

Fig. S5 XRD patterns of the contrast samples with different ratio of surfactant. (b) XRD patterns of the samples with different mole ratios of the metal salts.

Explanation about fitting the XRD pattern by calculating the peak density

In this work, Besides the strong peaks indexed to the Ni foam substrate (2 theta=44.59°, 51.90°, 76.56°) in the XRD pattern of flower like $Zn_{0.76}Co_{0.24}S/Co_3S_4$, the intensity ratio of obvious diffraction peaks of the composites at 28.64°, 33.28°, 47.65°, and 56.62° is 3036: 198: 1220:706, corresponding with the JCPDS card of 100: 7: 49: 26. ($Zn_{0.76}Co_{0.24}S$, No. 47-1656, space group: F-43m (216), a_0=5.3941 Å; b_0=5.3941 Å; c_0=5.3941 Å) And intensity ratio of the peaks at 31.36°, 50.23°, 55.30° is 314:181:243, corresponding with the JCPDS care of 100:70: 90. (Co_3S_4, No. 42-1448, space group: Fd3m (227), a_0=9.437 Å; b_0=9.437 Å; c_0=9.437 Å) This results are further evidence that the electrode materials compose of two metal sulfides. Similar to that of the flower like $Zn_{0.76}Co_{0.24}S/Co_3S_4$, the grass like $Zn_{0.76}Co_{0.24}S/Co_3S_4$ also includes the components of $Zn_{0.76}Co_{0.24}S$ and Co_3S_4.

Analyzing the synthesis of the composite in a simple way

The controlled experiments using different mole ratios of zinc and cobalt sources also have been done, which show a different result compared with the composite in the manuscript. (Fig. S5b) When there is only the source of cobalt, the product shows a XRD pattern of Co_3S_4. With the zinc and cobalt ratio of 3:1 or 3:0.5, the products also are composites of $Zn_{0.76}Co_{0.24}S$ and Co_3S_4. The mole ratio of the metal salts could be one of the reasons why the products are $Zn_{0.76}Co_{0.24}S/Co_3S_4$ rather than the solely $Zn_{0.76}Co_{0.24}S$. But there is not a definite answer on the complicated environment in present.

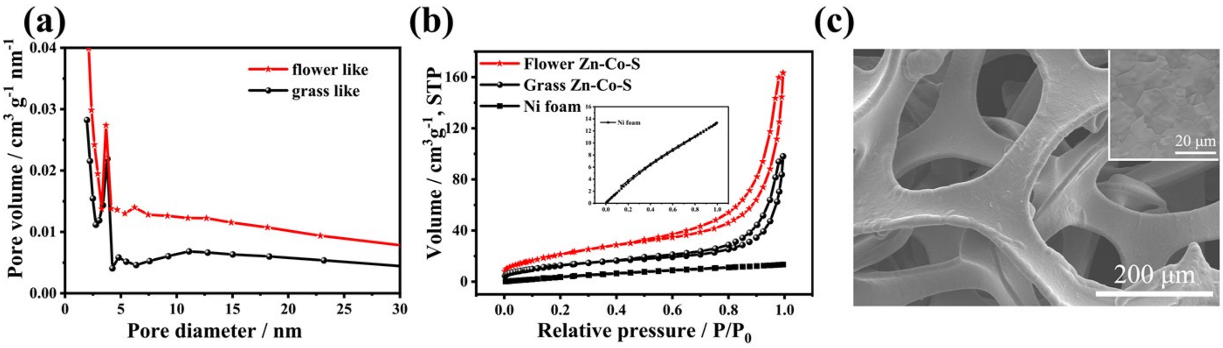

Fig. S6 (a)Barrett-Joyner-Halenda (BJH)-derived pore size distribution diagrams of flower and grass like $Zn_{0.76}Co_{0.24}S/Co_3S_4$. (b) N_2 adsorption/desorption isotherms of Ni foam compared with the electrode materials. (c) The SEM image of the pristine Ni foam without electrode materials.

Detailed method about the BET test

To maintain the self-supported morphologies of the electrodes and get the accurate results, we test the BET of all samples by the same method of putting the whole electrodes which include the Ni foam and electrode materials in the instrument.

Furthermore, the pore size of the samples mainly concentrate on the nanoscale. The pores in the Ni foam are about 200 μm which cannot influence the pore size distribution. (Fig. S6b, S6c)

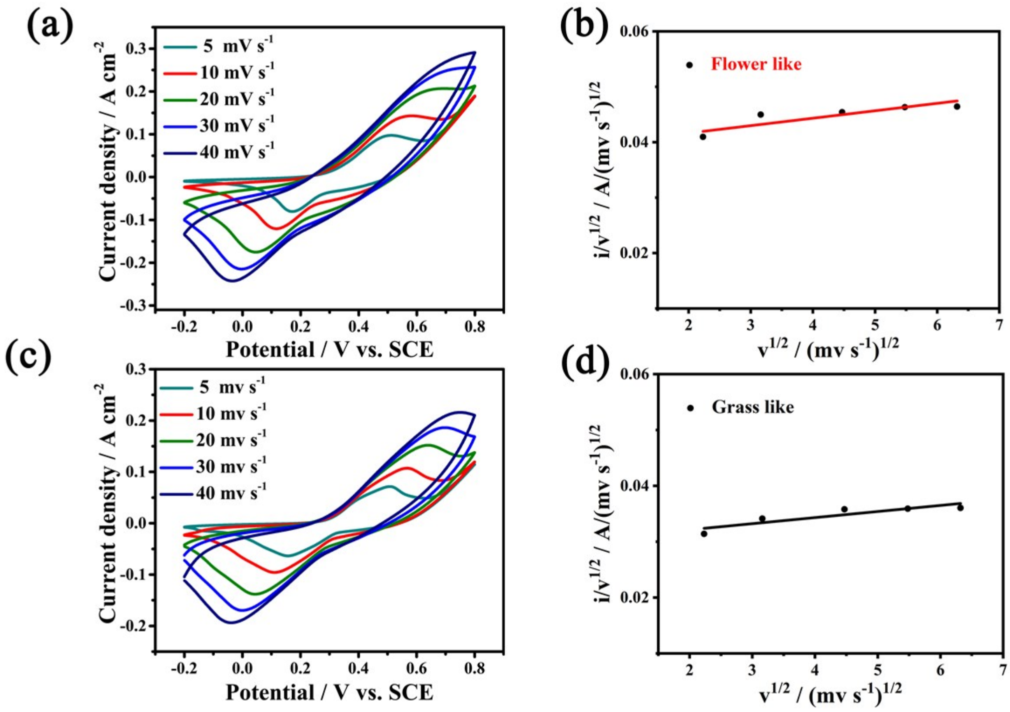

Fig. S7 (c) CV curves at different scan rates and (d) relation between the peak current and the scan rate for flower like $Zn_{0.76}Co_{0.24}S/Co_3S_4$. (c) CV curves at different scan rates and (d) relation between the peak current and the scan rate for grass like $Zn_{0.76}Co_{0.24}S/Co_3S_4$.

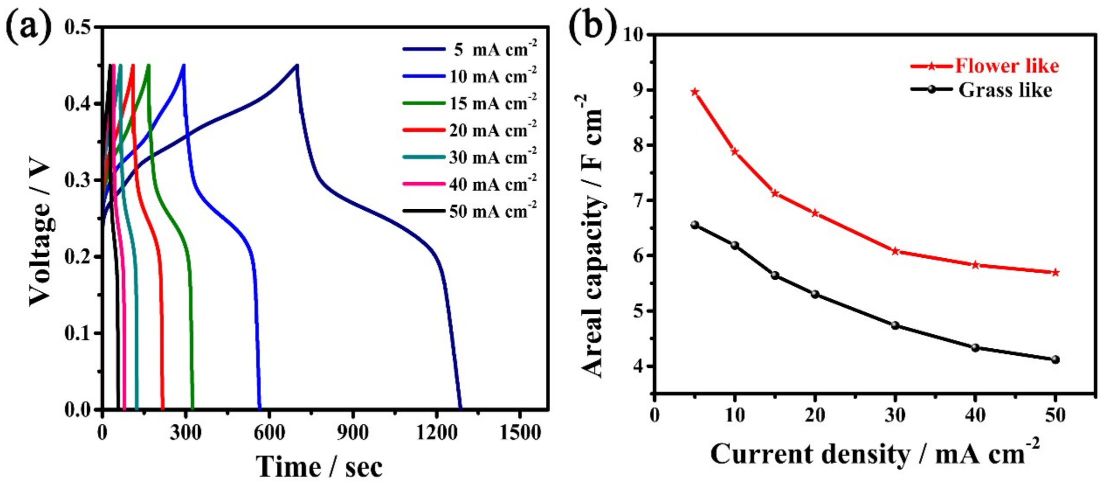

Fig. S8 (a) GCD curves of of grass like $Zn_{0.76}Co_{0.24}S/Co_3S_4$ at different current densities, (b) the C_{AC} comparison of the two electrode.

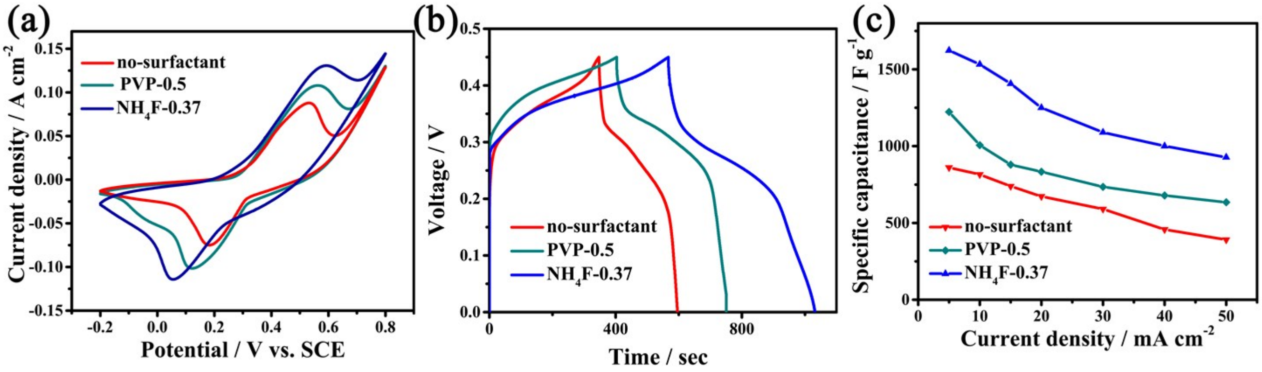

Fig. S9 (a) CV curves of contrast samples at 20 mV s^{-1}, (b) GCD curves of contrast samples at 5mA cm^{-2}, (c) the corresponding specific capacitance of contrast samples at different current density.

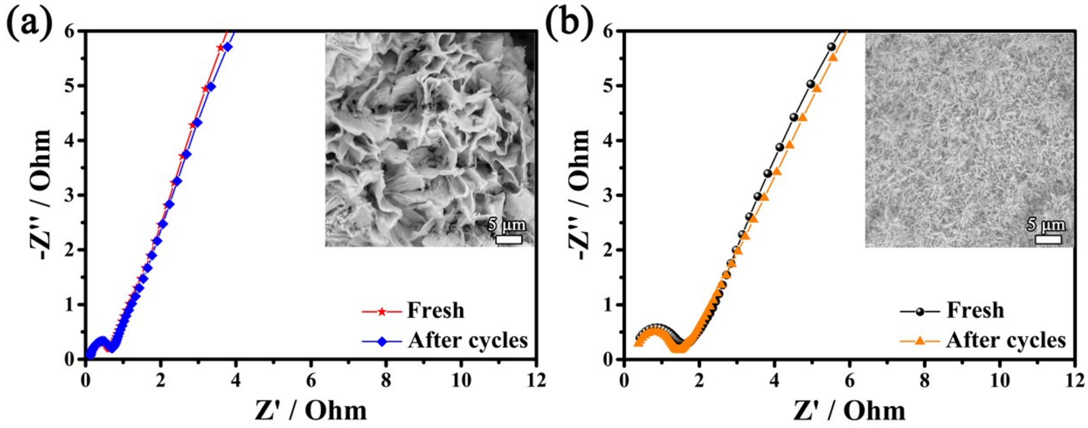

Fig. S10 (a) EIS and SEM images (inset) of the flower like $Zn_{0.76}Co_{0.24}S/Co_3S_4$ after cycles, (b) EIS and SEM images (inset) of the grass like $Zn_{0.76}Co_{0.24}S/Co_3S_4$ after cycles.

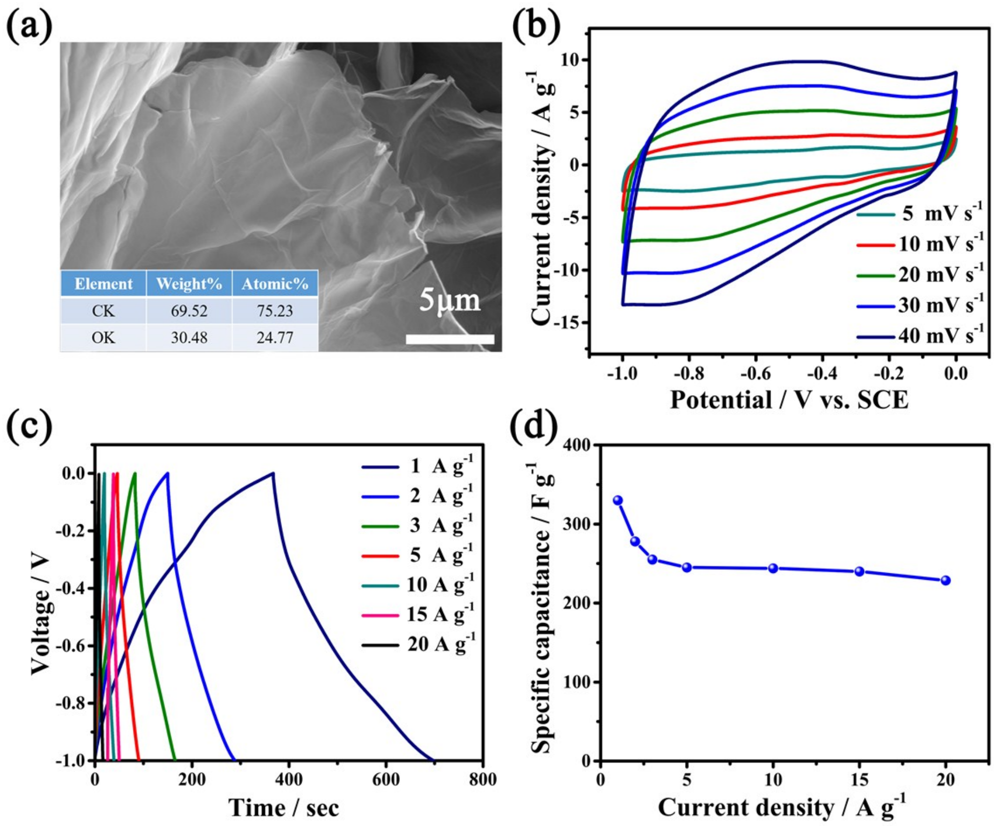

Fig. S11 (d) SEM image of RGO, (a) CV curves of RGO at different scan rates (from 5 to 40 mV s^{-1}), (b) GCD curves of RGO at various current densities (from 1 to 20 A g^{-1}), (c) specific capacitance versus current density of RGO.

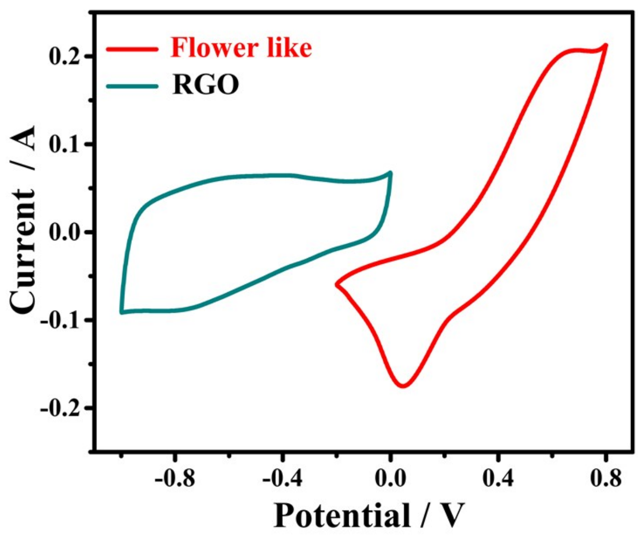

Fig. S12 CV curves of flower like $Co_3S_4/Zn_{0.76}Co_{0.24}S$ and RGO measured at a scan rate of 20 mV S^{-1} in a three-electrode system.

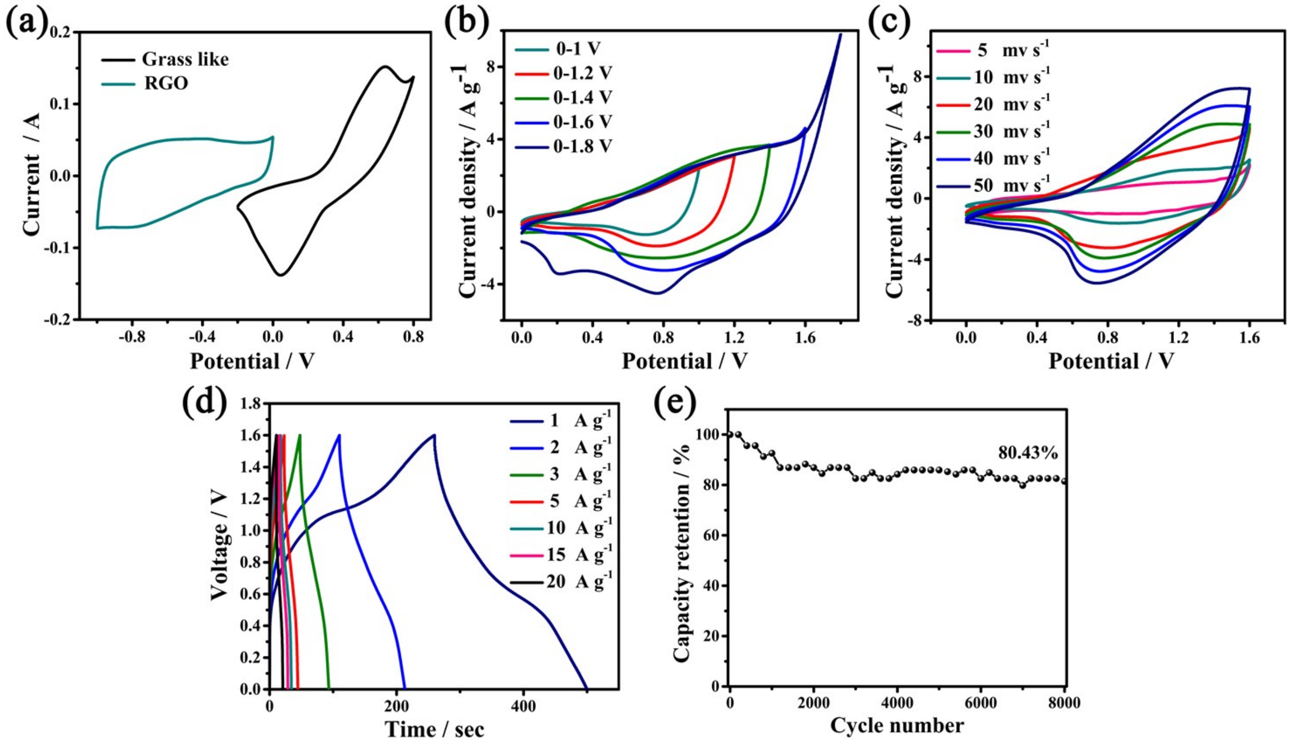

Fig. S13 a) CV curves of grass like $Co_3S_4/Zn_{0.76}Co_{0.24}S$ and RGO measured at a scan rate of 20 mV S^{-1} in a three-electrode system, b) CV curves of the grass like $Co_3S_4/Zn_{0.76}Co_{0.24}S$//RGO ASC measured at different potential window at 20mV S^{-1}, c) CV curves measured at different scan rates in a potential window of 1.6V, d) GCD curves of grass like $Co_3S_4/Zn_{0.76}Co_{0.24}S$//RGO ASC at different current densities, e) cycling performance of grass like $Co_3S_4/Zn_{0.76}Co_{0.24}S$//RGO ASC measured at 6A g^{-1} with 8000 cycles.

Table S1. The equations based on CV curves of flower and grass like $Zn_{0.76}Co_{0.24}S/Co_3S_4$.

Cathodic	$\mathbf{i/v^{1/2}=k_1v^{1/2}+k_2}$
Flower like $Zn_{0.76}Co_{0.24}S/Co_3S_4$	$i/v^{1/2}=0.001337v^{1/2}+0.03742$
Grass like $Zn_{0.76}Co_{0.24}S/Co_3S_4$	$i/v^{1/2}=0.000897v^{1/2}+0.03099$

Table S2. Comparison of electrochemical performances of the other electrode materials with present work in a three-electrode system.

Electrode materials	Areal capacitance	Specific capacitance	Electrolyte	Cyclic Stability	References
Flower like $Zn_{0.76}Co_{0.24}S/Co_3S_4$	8.96 F cm^{-2} at 5 mA cm^{-2}	2798.61 F g^{-1} at 1.56 A g^{-1}	6 M KOH	93.8% [7000]	This work
Grass like $Zn_{0.76}Co_{0.24}S/Co_3S_4$	6.56 F cm^{-2} at 5 mA cm^{-2}	2048.61 F g^{-1} at 1.56 A g^{-1}	6 M KOH	89.2% [7000]	This work
$Zn_{0.76}Co_{0.24}S$ nanosheets	-	2354.3 F g^{-1} at 1 A g^{-1}	1 M KOH	83.3% [1000]	1
$Zn_{0.76}Co_{0.24}S$ nanoartichokes	-	486.2 F g^{-1} at 2 A g^{-1}	1 M KOH	86.4% [2000]	2
$Zn_{0.76}Co_{0.24}S/Ni(OH)_2$ hollow nanotube	15.1 F cm^{-2} at 7 mA cm^{-2}	2157 F g^{-1} at 1 A g^{-1}	6 M KOH	78% [10000]	3
$Co_3S_4/CoMo_2S_4$		1457.8 F g^{-1} at 1 A g^{-1}	3 M KOH	97% [2000]	4
rGo-CNT-Co_3S_4		977 F g^{-1} at 1 A g^{-1}	6 M KOH	88.2% [5000]	5
$ZnCo_2O_4$ thin sheets	3.07 F cm^{-2} at 1 mA cm^{-2}	-	6 M KOH	96.3% [5000]	6
$ZnCo_2O_4$ flower		1657 F g^{-1} at 1 A g^{-1}	2 M KOH	82% [5000]	7
Caterpillar-like $NiCo_2O_4$		1777 F g^{-1} at 1 A g^{-1}	5 M KOH	83% [3000]	8
$ZnCo_2O_4/NiMoO_4$	6.07 F cm^{-2} at 2 mA cm^{-2}	1480.48 F g^{-1} at 0.5 A g^{-1}	6 M KOH	90.6% [15000]	9
$ZnCo_2O_4@MnO_2$	2.38 F cm^{-2} at 6 mA cm^{-2}	1981 F g^{-1} at 5 A g^{-1}	1 M KOH	90% [5000]	10
NiCo-LDH@NiOOH	-	2622 F g^{-1} at 1 A g^{-1}	6 M KOH	88.5% [10000]	11
$CuCo_2S_4$		1852 F g^{-1} at 2 A g^{-1}	2 M KOH	96% [4000]	12
$FeCo_2S_4$- $NiCo_2S_4$ composite	3.5 F cm^{-2} at 5 mA cm^{-2}	1519 F g^{-1} at 5 mA cm^{-2}	3 M KOH	95.1% [5000]	13
$FeCo_2S_4$		2411 F g^{-1} at 5 mA cm^{-2}	3 M KOH	92.2% [5000]	14

Discussion on the interaction between the $Zn_{0.76}Co_{0.24}S$ andCo_3S_4

There is only a conjecture about how the $Zn_{0.76}Co_{0.24}S$ hybrid with Co_3S_4, which is really a big challenge since the structure of hybrid composite materials is generally complicated. What's more the hybrid is not as simple as the mixture of two components physically. Both the interaction and interface between the two components should be considered for understanding the mechanism. In our view, it can surmise that the Zn^{2+} or Co^{2+} in $Zn_{0.76}Co_{0.24}S$ maybe share S^{2-} with the Co^{3+} or Co^{2+} in Co_3S_4, in which ion-electron-transfer would achieve between the two components during charging/discharging process. Meanwhile, the introduce of Co_3S_4 would reduce the internal resistance (R_s) of $Zn_{0.76}Co_{0.24}S$ and the grain boundary influence.

Meantime, it is found from the previous work (Adv. Energy Mater., DOI:10.1002/aenm.201702014), although the single $Zn_{0.76}Co_{0.24}S$ nanowires shows larger specific surface area (65.34 m^2/g) than that of grass like $Zn_{0.76}Co_{0.24}S/Co_3S_4$ (39.31 m^2/g) in this work, the R_S value of our composite (0.40 Ω for grass like sample) is much lower than that of the single $Zn_{0.76}Co_{0.24}S$. (1.13 Ω) due to the merits of $Zn_{0.76}Co_{0.24}S$ hybrid with Co_3S_4, which again provide the hint that interaction between the two components show more influence in electrochemical properties.

In this work, we have also done the contrast experiments and discovered that the individual part of Co_3S_4 deliver a lower specific capacitance (1052.96 F g^{-1} at 5 mA cm^{-2}) compared with the $Zn_{0.76}Co_{0.24}S/Co_3S_4$ (2798.16 F g^{-1} at 5 mA cm^{-2}), as shown in Fig. 5. There is a plain explain that the individual part of $Zn_{0.76}Co_{0.24}S$ or Co_3S_4 cannot deliver a specific capacitance as high as the $Zn_{0.76}Co_{0.24}S/Co_3S_4$. (J. Mater. Chem. A, 2016, 4, 18857-18867) So the $Zn_{0.76}Co_{0.24}S$ improves the specific capacitance of hybrid in the electrochemical test.

The synergistic effect of the two components is intricate and it is really complicated to discuss the role and mechanism of each component separately. In present, there are many works about the composite of metallic sulfide hybrids in the applications of energy storage, (J. Mater. Chem. A, 2017, 5, 133-144; Nanoscale, 2018, 10, 14171-14181; ACS Appl. Mater. Interfaces, 2017, 9, 12574-12583) but the interaction between the components has not been revealed completely which would be a significant research field in future.

In a short conclusion, it is complicate and incomplete to investigate the role of each component in affecting the electrochemical properties individually instead of considering two components as a hybrid with synergistic interaction. The detail and deep understanding of interaction need more direct proofs and further study.

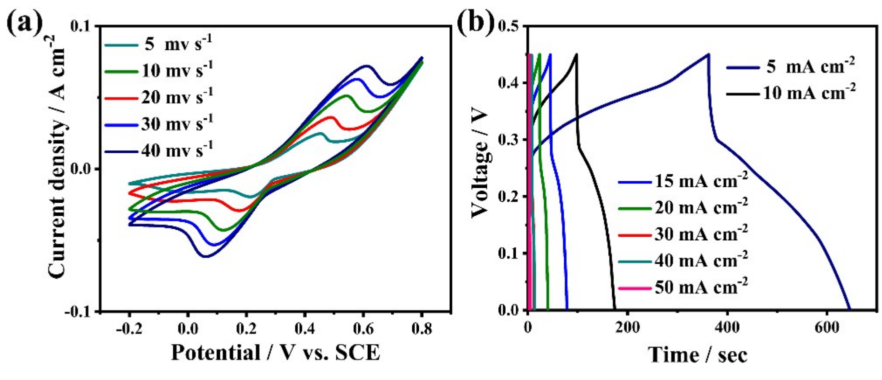

Fig. S13 The electrochemical performance of the Co_3S_4.

Table S3. Comparison of other asymmetric supercapacitors and present work.

Device	Electrolyte	Device window	Energy density	Power density	Cyclic Stability	References
Flower like $Zn_{0.76}Co_{0.24}S/Co_3S_4$ // RGO	KOH/PVA	1.6 V	62.22 Wh kg^{-1}	800 W kg^{-1}	86.29% [8000]	This work
Branch like $Zn_{0.76}Co_{0.24}S/Co_3S_4$ // RGO	KOH/PVA	1.6 V	55.56 Wh kg^{-1}	800 W kg^{-1}	80.43% [8000]	This work
Zn-Co-S nanosheets // AC	KOH/PVA	1.7 V	31.9 Wh kg-1	850 W kg-1	71% [10000]	1
$Co_3S_4/CoMo_2S_4$ // AC	3 M KOH	1.7 V	33.1 Wh kg^{-1}	850 W kg^{-1}	93.8% [5000]	4
rGo-CNT-Co3S4 // NGN	6 M KOH	1.6 V	43.5 Wh kg^{-1}	400 W kg^{-1}	90% [3000]	5
ZnCo2O4 thin sheets // AC	6 M KOH	1.7 V	36.31 Wh kg^{-1}	850 W kg^{-1}	92.5% [10000]	6
ZnCo2O4/NiMoO4 // AC	6 M KOH	1.6 V	48.6 Wh kg^{-1}	100 W kg^{-1}	94% [3000]	9
NiCo-LDH@NiOOH // AC	6 M KOH	1.5 V	51.7 Wh kg^{-1}	599 W kg^{-1}	77.6% [10000]	11
CoS/graphene // AC	2 M KOH	1.6 V	29 Wh kg^{-1}	800 W kg^{-1}	70% [10000]	15
$ZnCo_2O_4$@ $NixCo_{2x}(OH)_{6x}$ // AC	2 M KOH	1.7 V	26.2 Wh kg^{-1}	511.8 W kg^{-1}	88.2% [2000]	16
NiCo2S4@Co(OH)2 // AC	2 M KOH	1.6 V	35.89 Wh kg^{-1}	400 W kg^{-1}	70% [5000]	17
CuCo2O4/CuO // RGO/Fe2O3	2 M KOH	1.6 V	33 Wh kg^{-1}	200 W kg^{-1}	83% [5000]	18

The detailed analysis about the mechanism of the ASC

The positive material ($Zn_{0.76}Co_{0.24}S/Co_3S_4$) is a kind of typical pseudocapacitive material and provide a super-high specific capacitance (2798.16 F g^{-1}) which originates from the invertible redox reactions on the electrode surface, which can drastically improve the energy density of the asymmetric supercapacitors.

RGO serves as negative material and works in a large potential (1.0 V) compared with the positive material (0.45 V) in the same electrolyte, which can improve the potential window of the devices effectively. As the traditional electric double layer capacitive materials, RGO gives a high rate capability and maintains the high power density of the device.

The electrode materials ($Zn_{0.76}Co_{0.24}S/Co_3S_4$//RGO) working in different voltage ranges further widen the potential window of the assembled asymmetric supercapacitors up to 1.6V compared with the symmetric device (1V).

And the proper mass ratio of the positive and negative materials was calculated by the equation according to the charge balance, which can make the two electrode play a full role in the device and get a high device capacitance (175 F g^{-1}).

From the equation of calculating the energy density, it is discovered that the device capacitance and potential window greatly affect the energy density of the device.

$$E=CV^2/2$$

Where E is the energy density, C is the device capacitance, and V is the cell voltage.

Consequently, the $Zn_{0.76}Co_{0.24}S/Co_3S_4$//RGO asymmetric supercapacitors with wide potential window and a high device capacitance deliver a high energy and power densities.

Notes and references

1. K. Tao, X. Han, Q. Cheng, Y. Yang, Z. Yang, Q. Ma and L. Han, *Chem-Eur. J.*, 2018, **24**, 1800960.
2. J. Yang, Y. Zhang, C. Sun, G. Guo, W. Sun, H. Wei, Q. Yan and X. Dong, *J. Mater. Chem. A*, 2015, **3**, 11462-11470.
3. J. A. Syed, J. Ma, B. Zhu, S. Tang and X. Meng, *Adv. Energy Mater.*, 2017, **7**, 1701228.
4. X. Yang, H. Sun, P. Zan, L. Zhao and J. Lian, *J. Mater. Chem. A*, 2016, **4**, 18857-18867.
5. A. Mohammadi, N. Arsalani, A. G. Tabrizi, S. E. Moosavifard, Z. Naqshbandi and L. S. Ghadimi, *Chem. Eng. J.*, 2018, **334**, 66-80.
6. J. Zhu, D. Song, T. Pu, J. Li, B. Huang, W. Wang, C. Zhao, L. Xie and L. Chen, *Chem. Eng. J.*, 2018, **336**, 679-689.
7. G. Rajeshkhanna and G. R. Rao, *Electrochim. Acta*, 2018, **261**, 265-274.
8. X. Chen, D. Chen, X. Guo, R. Wang and H. Zhang, *ACS Appl. Mater. Interfaces*, 2017, **9**, 18774-18781.
9. J. Hong, Y. -W. Lee, D. Ahn, S. Pak, J. Lee, A. -R. Jang, S. Lee, B. Hou, Y. Cho and S. M. Morris, H. S. Shin, S. Cha, J. I. Sohn and J. M. Kim, *Nano Energy*, 2017, **39**, 337-345.
10. W. Ma, H. Nan, Z. Gu, B. Geng and X. Zhang, *J. Mater. Chem. A*, 2015, **3**, 5442-5448.
11. H. Liang, J. Lin, H. Jia, S. Chen, J. Qi, J. Cao, T. Lin, W. Fei and J. Feng, *J. Power Sources*, 2018, **378**, 248-254.
12. Y. Wang, D. Yang, T. Zhou, J. Pan, T. Wei and Y. Sun, *Nanotechnology*, 2017, **28**, 465402.
13. J. Zhu, S. Tang, J. Wu, X. Shi, B. Zhu and X. Meng, *Adv. Energy Mater.*, 2017, **7**, 1601234.
14. S. Tang, B. Zhu, X. Shi, J. Wu and X. Meng, *Adv. Energy Mater.*, 2017, **7**, 1601985.
15. J. Shi, X. Li, G. He, L. Zhang and M. Li, *J. Mater. Chem. A*, 2015, **3**, 20619-20626.
16. W. Fu, Y. Wang, W. Han, Z. Zhang, H. Zha and E. Xie, *J. Mater. Chem. A*, 2015, **4**, 173-182.
17. R. Li, S. Wang, Z. Huang, F. Lu and T. He, *J. Power Sources*, 2016, **312**, 156-164.
18. Y. Wang, C. Shen, L. Niu, R. Li, H. Guo, Y. Shi, C. Li, X. Liu and Y. Gong, *J. Mater. Chem. A*, 2016, **4**, 9977-9985.